eLIFE elifesciences.org

RESEARCH ARTICLE

Figures and figure supplements

Resistome diversity in cattle and the environment decreases during beef production

Noelle R Noyes *et al*

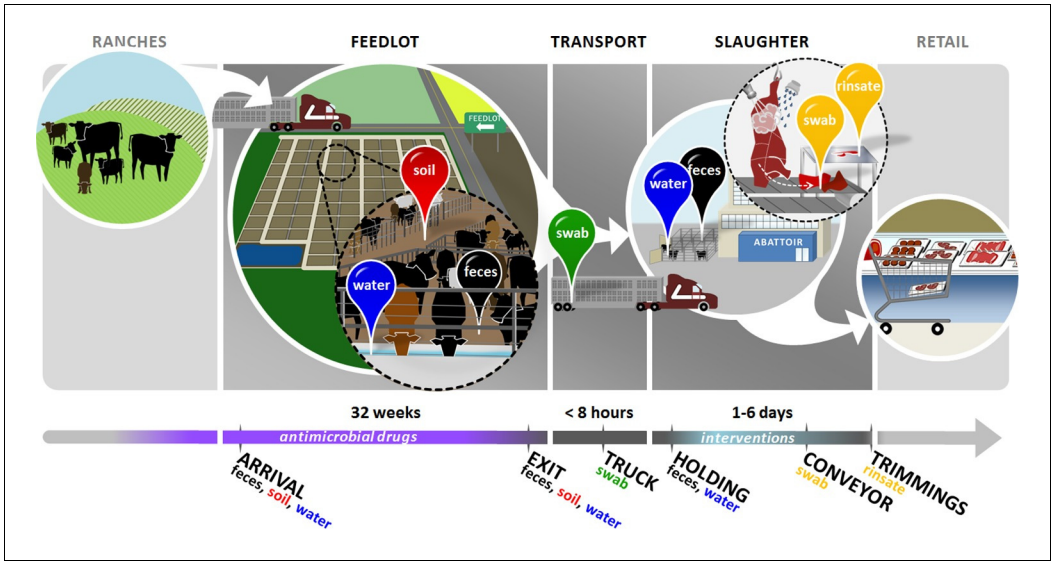

Figure 1. Overview of sampling design. Cattle in this study were born on ranches and entered the feedlots between 3 and 12 months of age. In the feedlots, we collected pooled fecal (black pin), soil (red pin), and drinking water (blue pin) samples from 2 pens of cattle in each of 4 feedlots. These samples were collected once around the time that study cattle arrived in the feedlot ('arrival'), and then once when the same cattle had reached slaughter weight and were ready to exit the feedlot ('exit'). Study cattle were then loaded onto transport trucks for shipment to the abattoir. Pooled swabs (green pin) from the inside walls of the transport trucks were collected immediately after the cattle had been unloaded at the abattoir ('truck'). Cattle were then placed into a holding pen outside of the abattoir, where pooled fecal (black pin) and drinking water (blue pin) samples were collected ('holding'). Cattle then entered the abattoir, where they were humanely slaughtered and their carcasses disassembled into beef products for retail. At the end of this process, we collected swabs (yellow pin) from the conveyor belts used to move carcass parts ('conveyor'), as well as rinsates (yellow pin) of the carcass trimmings used to make ground beef ('trimmings'). See ***Figure 1—source data 1*** for sampling details, including exact sampling dates for all 8 pens in this study.

DOI: 10.7554/eLife.13195.003

The following source data is available for figure 1:

Source data 1. Sample collection details, by location, sample matrix and pen.

DOI: 10.7554/eLife.13195.004

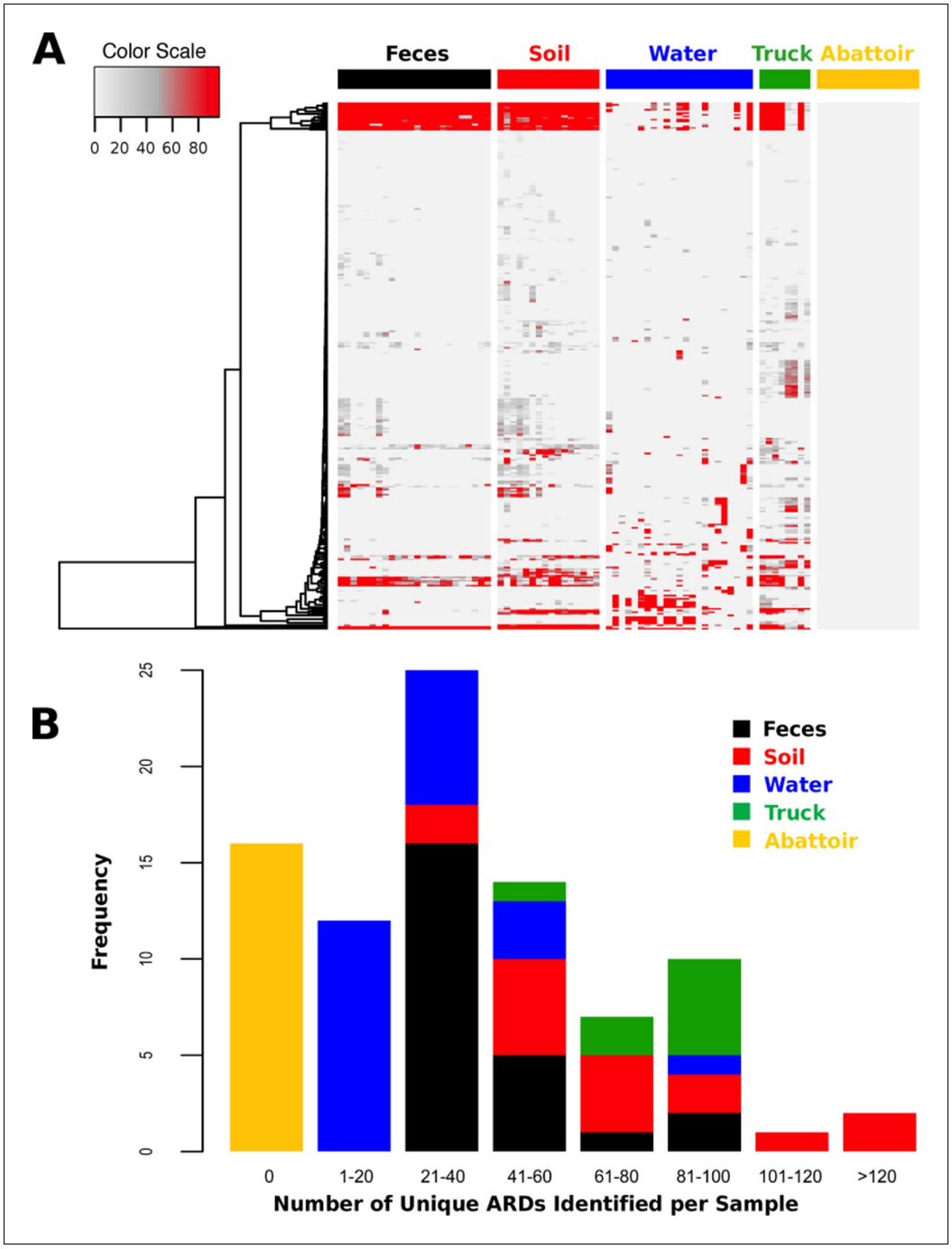

Figure 2. ARD abundance and frequency, by sample type. (**A**) Heatmap of the 319 ARDs (rows) identified in 87 samples (columns) collected from the beef production system. Columns are grouped by sampling location but are unclustered. ARDs are clustered along rows using Euclidean distances with complete linkage. ARD names by row can be viewed in the source data for ***Figure 2***. Color scale values indicate the number of normalized alignments per ARD per sample. (**B**) Histogram of unique ARDs identified per sample (N=87). See ***Figure 2—source data 1*** for raw count matrix of ARDs by sample, which was used to produce heatmap and histogram.

DOI: 10.7554/eLife.13195.006

The following source data is available for figure 2:

Source data 1. Raw and normalized count matrix of ARDs (rows) identified by sample (columns).

DOI: 10.7554/eLife.13195.007

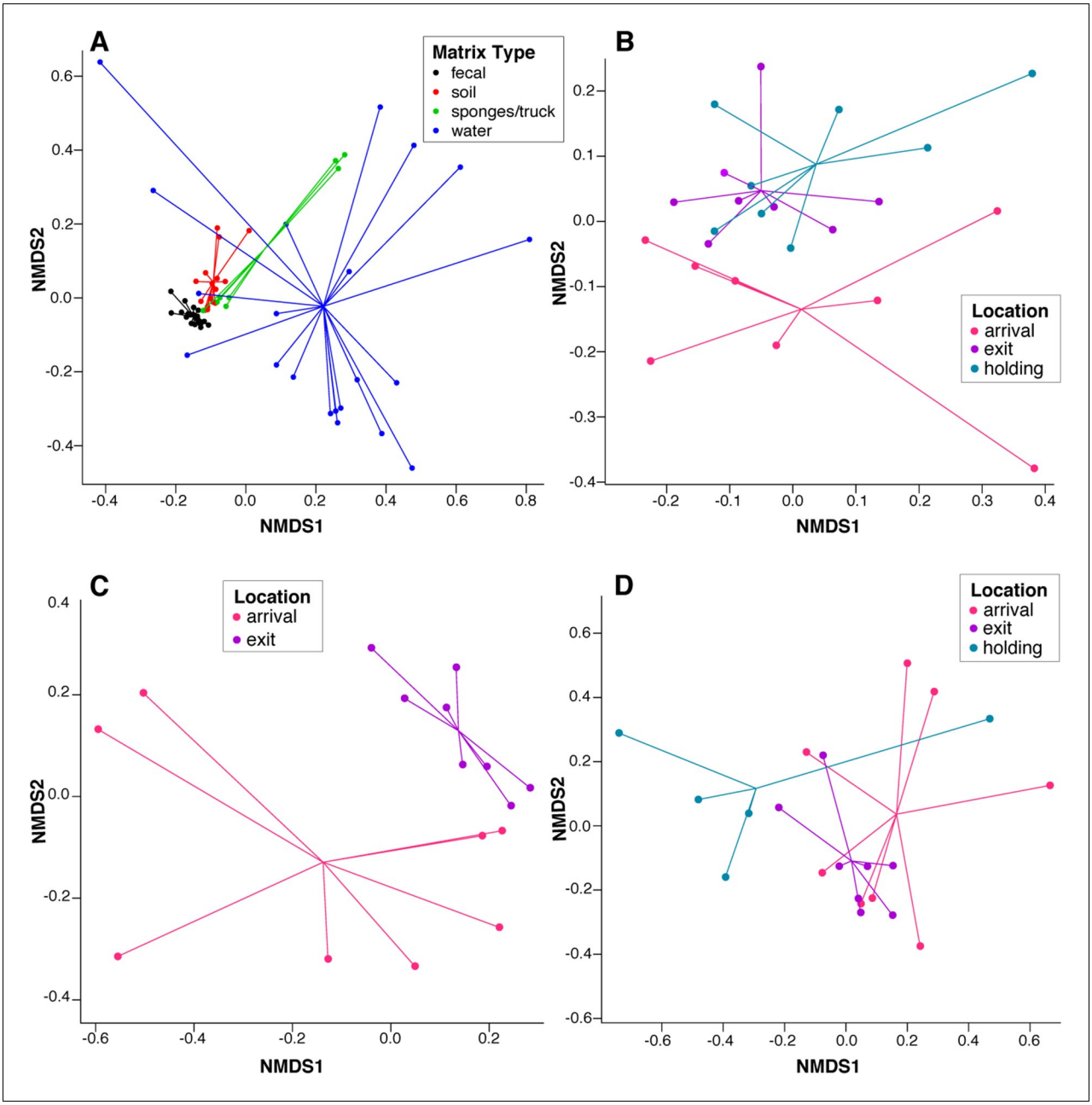

Figure 3. NMDS ordination plots of ARD composition, by sample type and location. Non-metric multidimensional scaling (NMDS) ordination plots of pre-slaughter sample ARD composition, depicting significant sample separation by (**A**) matrix (Stress=0.13, R=0.41, p=0.001), and location within (**B**) feces (Stress = 0.10, R=0.03, p=0.04), (**C**) soil (Stress = 0.05, R=0.34, p=0.006) and (**D**) water (Stress=0.10, M=0.29, p=0.005).
DOI: 10.7554/eLife.13195.008

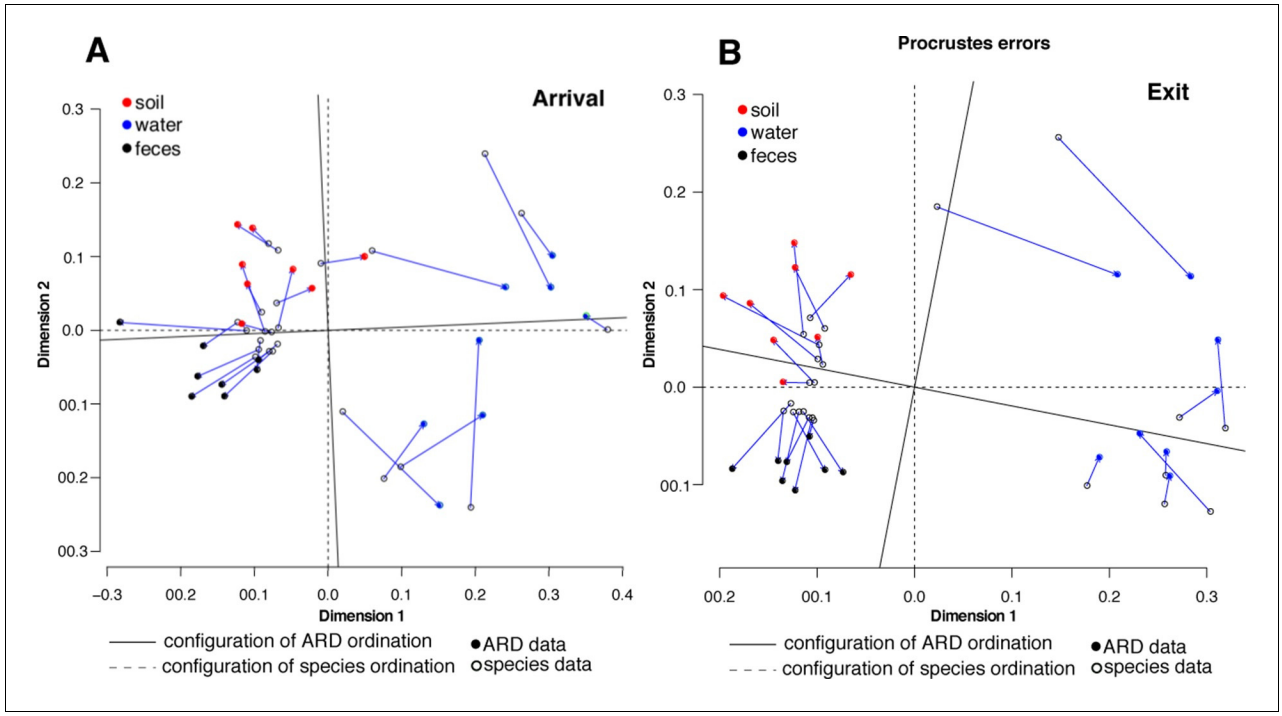

Figure 4. Procrustes analysis of ARD content (filled circles) and species composition (open circles) at arrival (**A**) and exit (**B**) using Hellinger transformation and NMDS ordination (***Legendre and Gallagher, 2001***). Stress values for ARD ordination at arrival and exit were 0.08 and 0.03, respectively, and for microbiome species ordination at arrival and exit were 0.06 and 0.07, respectively. Soil (red), water (blue) and fecal (black) samples clustered significantly in the microbiome and resistome data. Procrustes configurations were correlated in the arrival and exit samples, but less so in the exit samples (M^2 = 0.29 and 0.18, respectively).

DOI: 10.7554/eLife.13195.009

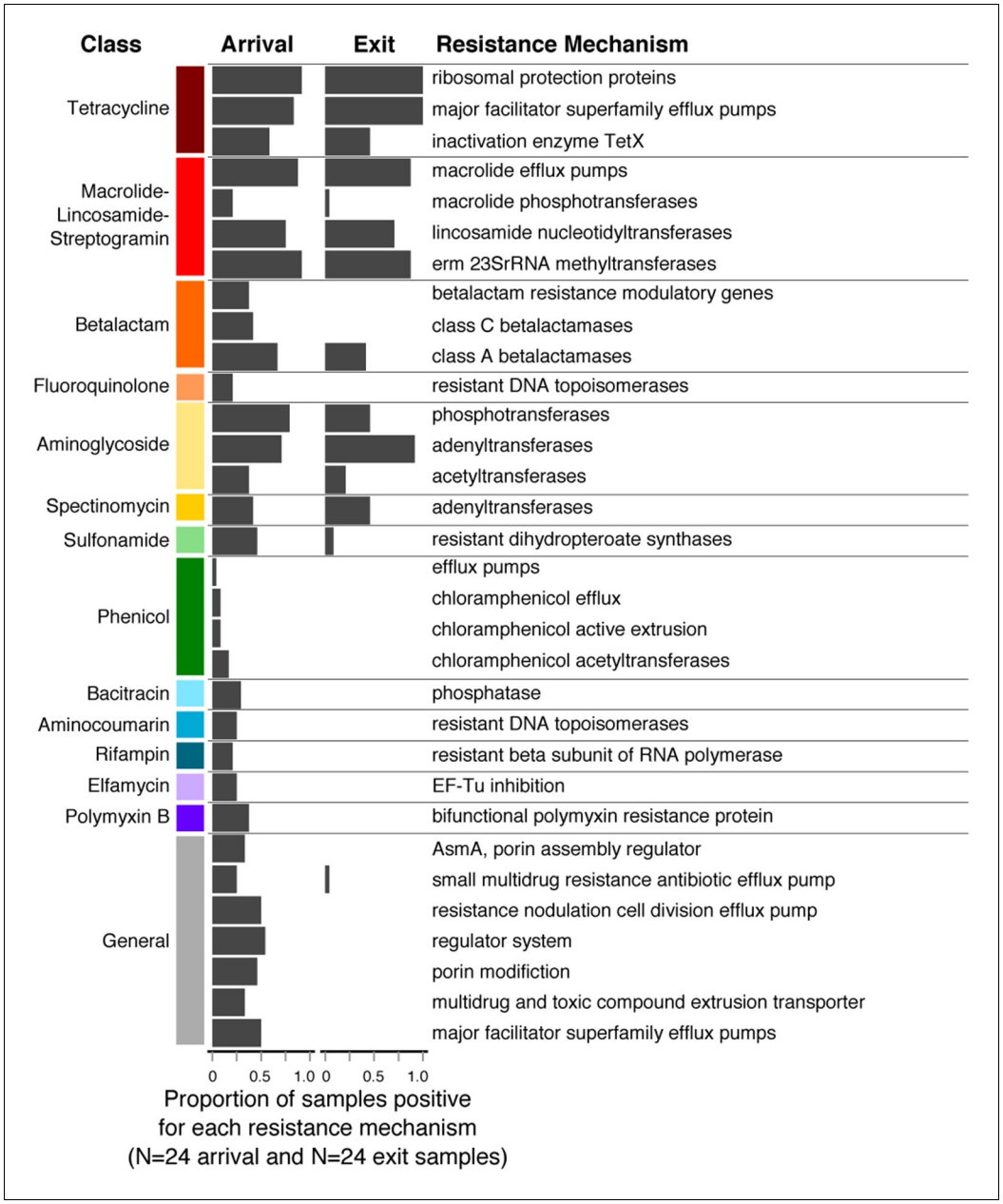

Figure 5. Changes in prevalence of resistance mechanisms during the feedlot period (arrival to exit). Proportion of arrival (n=8 soil, 8 fecal, 8 water) and exit (n=8 soil, 8 fecal, 8 water) samples that contained at least one ARD in each resistance mechanism (n=33), grouped by resistance class.

DOI: 10.7554/eLife.13195.010

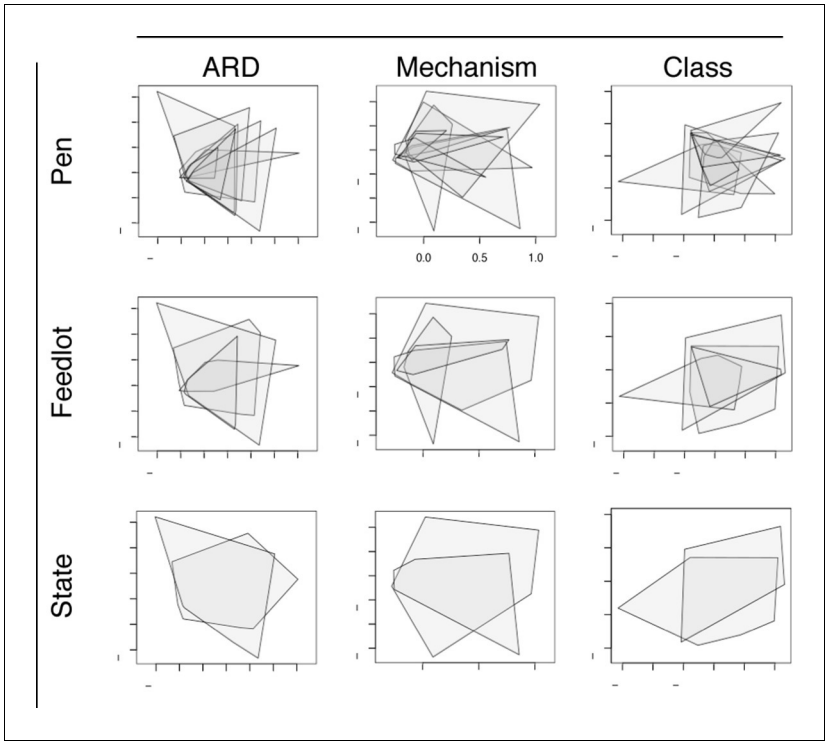

Figure 6. Non-metric multidimensional scaling (NMDS) ordination plots at the ARD, mechanism and class levels, visualized by pens (n=8), feedlots (n=4) and states (n=2). In each NMDS plot, a polygon corresponds to one unit (i.e., pen, feedlot or state) and represents the convex hull for that unit (i.e. the smallest amount of space within the graph that contains all points (or samples) within that unit). To view results of NMDS ordination, as well as adonis and anosim statistics, see ***Figure 6—source data 1***.

DOI: 10.7554/eLife.13195.012

The following source data is available for figure 6:

Source data 1 NMDS ordination, adonis, and anosim results at the ARD, mechanism and class levels, by pen, feedlot, and state variables.

DOI: 10.7554/eLife.13195.013

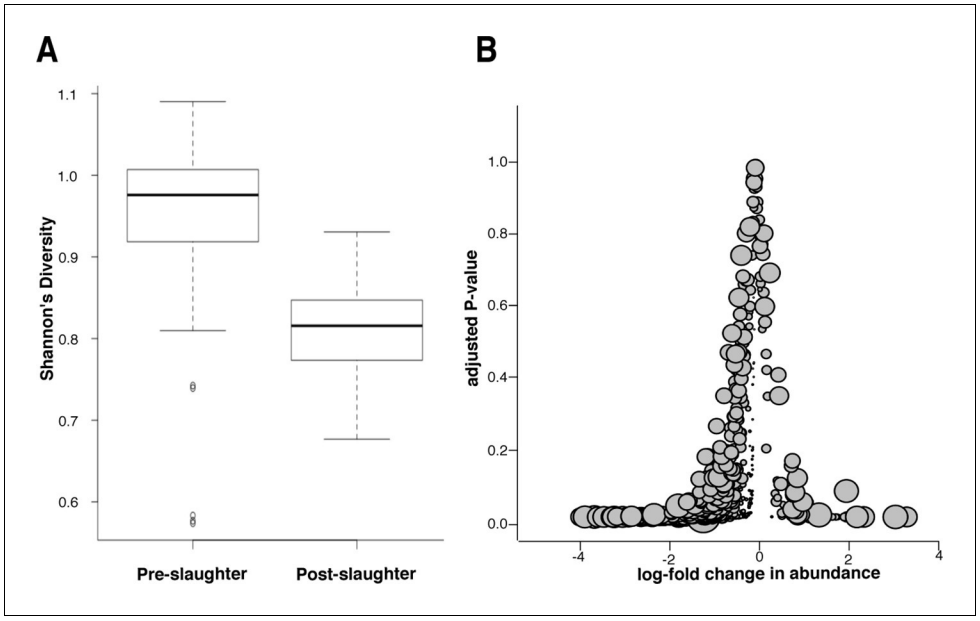

Figure 7. Microbiome changes from pre- to post-slaughter in all samples. (**A**) Boxplot of Shannon's diversity at the species level, pre- vs. post-slaughter across all sample matrices. Shannon's diversity was significantly lower in post-slaughter samples when tested using Wilcoxon paired rank test ($P<0.0001$). See source data for ***Figure 7*** (sheet '***Figure 7A***') for Shannon's Diversity Index by sample, which was used to produce boxplots. (**B**) Log_2-fold change in abundance of genera from pre- to post-slaughter versus adjusted *P*–value, across all samples matrices. Dot size is proportional to the average abundance of the genus across all samples. For taxa table and counts used to produce model of log_2-fold change in abundance, see ***Figure 7—source data 1*** (sheet '***Figure 7B*** taxa table'); for model output, see ***Figure 7—source data 1*** (sheet '***Figure 7B*** model output').

DOI: 10.7554/eLife.13195.014

The following source data is available for figure 7:

Source data 1. Shannon's diversity, taxa table and model output for ***Figure 7***.

DOI: 10.7554/eLife.13195.015

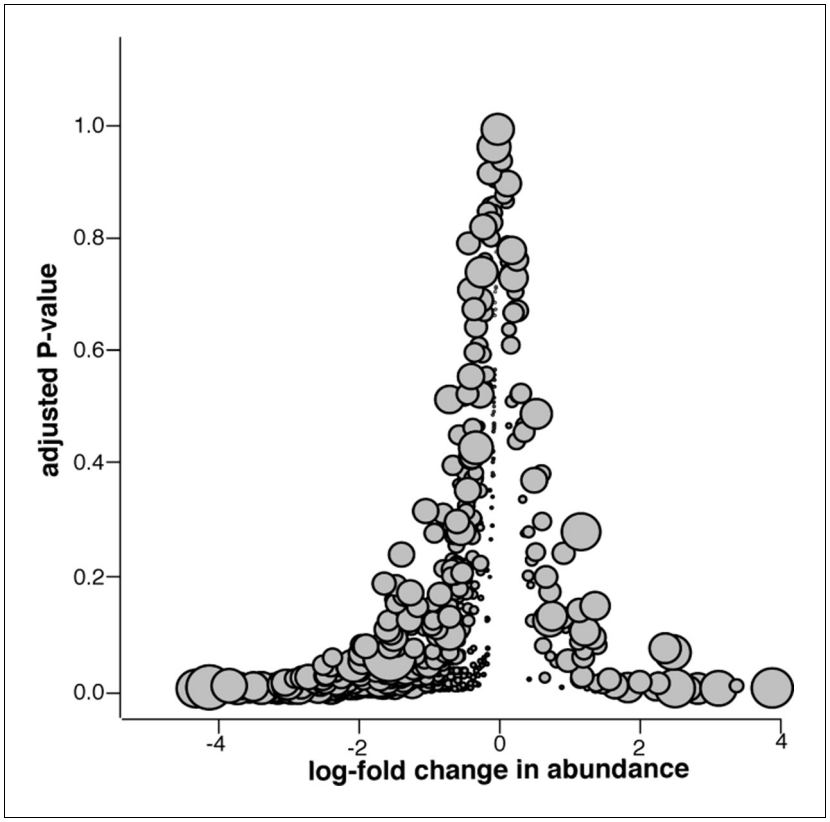

Figure 7—figure supplement 1. Microbiome changes from pre- to post-slaughter in swab samples only. Log_2-fold change in abundance of genera from pre- to post-slaughter versus adjusted *P*–value, using only swab samples. Dot size is proportional to the average abundance of the genus across all samples. See ***Figure 7—source data 1*** (sheet '***Figure 7*** supp. model output') to view model output for the genus-level analysis of log_2-fold change in abundance for swab samples only.

DOI: 10.7554/eLife.13195.016